Published in final edited form as:
J Am Chem Soc. 2010 August 11; 132(31): 10816–10822. doi:10.1021/ja1026858.

Single-molecule observation of protein adsorption onto an inorganic surface

David J. Niedzwiecki[1], **John Grazul**[2], and **Liviu Movileanu**[1,3,4]

[1]Department of Physics, Syracuse University, 201 Physics Building, Syracuse, New York 13244-1130, USA

[2]Cornell Center for Materials Research, Cornell University, 627 Clark Hall of Science, Ithaca, New York 14853, USA

[3]Structural Biology, Biochemistry, and Biophysics Program, Syracuse University, 111 College Place, Syracuse, New York 13244-4100, USA

[4]Syracuse Biomaterials Institute, Syracuse University, 121 Link Hall, Syracuse, NY 13244, USA

Abstract

Understanding the interactions between silicon-based materials and proteins from the blood stream is of key importance in a myriad of realms, such as design of nanofluidic devices and functional biomaterials, biosensors, and biomedical molecular diagnosis. By using nanopores fabricated in 20 nm-thin silicon nitride membranes and highly sensitive electrical recordings, we show single-molecule observation of nonspecific protein adsorption onto an inorganic surface. A transmembrane potential was applied across a single nanopore-containing membrane immersed into an electrolyte-filled chamber. Through the current fluctuations measured across the nanopore, we detected long-lived captures of bovine serum albumin (BSA), a major multifunctional protein present in the circulatory system. Based upon single-molecule electrical signatures observed in this work, we judge that the bindings of BSA to the nitride surface occurred in two distinct orientations. With some adaptation and further experimentation, this approach, applied on a parallel array of synthetic nanopores, holds potential for use in methodical quantitative studies of protein adsorption onto inorganic surfaces.

Keywords

Single-molecule Biophysics; Nanobiotechnology; Low-stress Silicon Nitride; Bovine Serum Albumin; Solid-state Nanopore; Liquid-solid Interface

INTRODUCTION

Spontaneous adsorption of proteins onto solid-state surfaces[1–3] is at the heart of a broad spectrum of areas, including biochip applications, nanomedical devices, and design of a new class of functional hybrid biomaterials. Despite many experimental studies on protein

Correspondence/reprint requests: Liviu Movileanu, PhD, Department of Physics, Syracuse University, 201 Physics Building, Syracuse, New York 13244-1130, USA; Phone: 315-443-8078; Fax: 315-443-9103; lmovilea@physics.syr.edu.

Supporting Information Available: Protocols for nanopore preparation and treatments, single-channel electrical recordings with solid-state nanopores, preparation of the silicon nitride membranes, the characterization of the nanopores, the tests for the BSA purity, the statistical details of the short-lived and long-lived current blockades, hints on the derivation of Eq. 1, the experimental evidence for the reproducibility of the long-lived current blockades using various nanopores, and the observation of short polypeptides with narrower solid-state nanopores are provided. This material is available free of charge via the Internet at http://pubs.acs.org.

adsorption at the liquid-solid interface,[1,2,4–8] this phenomenon is still not comprehensively understood. In general, protein adsorption is considered an irreversible nonspecific process,[4–6] where the occupied area remains excluded for other proteins in the aqueous phase, because proteins attached to the solid surface do not show lateral mobility or significant desorption rates.[6,8,9] The complexity of protein adsorption on solid surfaces results from the multitude of electrostatic and hydrophobic forces among the side chains of the proteins and the reactive groups at the solid-liquid interface.[9]

In this paper, we probe protein adsorption on a low-stress silicon nitride (Si_xN_y) surface at single-molecule resolution using the resistive-pulse technique.[10–12] In this technique, single-channel current measurements (Supporting Information)[13] are employed to detect, explore and characterize an analyte by measuring the fluctuations in a current signature produced by ions passing through a single nanopore. These fluctuations occur when the analyte partitions into the nanopore, excluding the volume available for ion passage, thus causing a decrease in the current. We employed solid-state nanopores (Supporting Information, Figs. S1–S3)[14,15] that feature an array of advantages, such as the robustness of the membrane and the ability to easily tune the diameter of the nanopore. Below, we describe time-resolved, long-lived captures of single bovine serum albumin (BSA), a 66.4 kDa-molecular mass protein, into a Si_xN_y -based nanopore. While such long-lived captures have been observed before,[16–18] to our knowledge, this is the first time they have been studied systematically.

The nanopores were drilled into a 20 nm-thin amorphous Si_xN_y film using a concentrated electron beam (Supporting Information, Fig. S1; Fig. 1).[19,20] Over 40 different nanopores were used, with diameters ranging from 3 to 25 nm. BSA, the most abundant protein in the bovine blood stream, is folded in a globular conformation with the approximate dimensions of 4 × 4 × 14 nm, giving it an excluded volume of ~224 nm^3.[21] When using nanopores of diameter greater than 8 nm, the addition of low nanomolar concentrations of BSA to the chamber produced transient short-lived current blockades in the range of 20 μs or shorter.

We show experimental evidence that the long-lived captures of single BSA proteins, in a broad range from tens of milliseconds to several minutes, are caused by nonspecific, random and spontaneous attachment of single proteins to the Si_xN_y surface within the nanopore interior. Each adsorbed BSA protein produces a discrete drop in the current measured through a single nanopore. We found that the resulting current state followed one of two patterns. Either it was a stable constant value for long periods, or it fluctuated. We judge that the current fluctuations were due to a movable, unattached part of BSA that does not show significant interactions with the Si_xN_y surface. The fluctuations of the resulting current state of the nanopore were voltage dependent and obeyed a simple energetic landscape that is tilted along the applied electric force.[22] When we used nanopores with a diameter of ~9 nm, a long-lived current drop was accompanied by an alteration of the frequency of short-lived current spikes. These short-lived spikes were attributed to BSA partitions into the nanopore interior without significant interactions of the protein with the Si_xN_y surface. On the contrary, the frequency of long-lived captures of BSA did not undergo a simple dependence on the protein concentration in aqueous phase. We interpret these events result from nonspecific, random and spontaneous adsorption of single BSA proteins to the Si_xN_y surface of the nanopore interior.[4–6]

RESULTS

The excluded volume of free BSA proteins

When a positive voltage was applied across the Si_xN_y membrane, a uniform, event-free single-nanopore current was recorded (Fig. 2A). With the addition of BSA to the *cis*

chamber, which was grounded (Supporting Information, Fig. S4), two types of interactions were observed: very short-lived current spikes and long-lived current blockades (Fig. 2B). As BSA has an effective negative charge of 12e at pH 7.4,23 it is expected that, at a positive potential, the electric field within the nanopore interior will drive the negatively charged BSA through the nanopore. Short-lived events occurred at positive, but not negative voltages, confirming that the BSA protein has a net negative charge under the conditions used in this work. Dwell times for these events were near the resolution of our setup (~15 μs) and did not conform to a simple exponential. These findings are in accord with previous experiments performed with solid-state nanopores and BSA.16,17,24 The amplitude of the short-lived current blockades varied significantly (Fig. 2B), suggesting that BSA traverses the nanopore under different structural conformations. The frequency of short-lived current blockades scaled linearly with the BSA concentration, confirming that single BSA proteins were the cause of the events (Supporting Information, Fig. S5–S6).

The average excluded volume (Λ) of the BSA proteins may be estimated using the following equation:25

$$\Lambda \cong \frac{\Delta I_b \left(H_{eff}\right)^2}{\sigma V} \tag{1}$$

which depends on the amplitude of the current blockade made by the BSA proteins (ΔI_b), the effective length of the nanopore (H_{eff}), the applied transmembrane potential (V), and the conductivity (σ) of the solution within the interior of the nanopore. It should be noted that this is an approximate equation in which the protein is assumed smaller than the diameter of the nanopore (Supporting Information). A typical maximum value of ΔI_b was 2500 pA. If we use this value, and σ = 112 mS/cm,25 V= +150 mV, and H_{eff}=20 nm, which is the thickness of the Si_xN_y membrane, then the expected excluded volume is $\Lambda \cong 595\ nm^3$. The events with an amplitude greater than 2000 pA were rare (< 1%), so that they might be attributed to a very low concentration of dimmers and trimers in the BSA sample (Supporting Information, Fig. S4). Using a value of 224 nm^3 for the excluded volume of BSA,21 we employ equation (1) to find that the expected amplitude of the current blockade $\Delta I_b \cong 941$ pA. It is worth mentioning that H_{eff} could be greater than 20 nm, if the applied electric field extends beyond the wall of the nanopore. The access resistance of the nanopore is ρ/d,26 where ρ is the resistivity of the KCl solution and d is the nanopore diameter. Under the experimental conditions used in this work, the access resistance of a nanopore with a diameter of 12 nm is 7.44×10^6 Ω. This value is of the same order of magnitude as the resistance of the nanopore (1.58×10^7 Ω), which was calculated using a cylindrical geometry. Therefore, we need to take into account the access resistance of the nanopore. This is equivalent to making the nanopore πd/4, or roughly 0.8d, longer.26 For a typical nanopore with a diameter of 12 nm, then the effective length H_{eff} is 29 nm, which gives $\Delta I_b \cong 429$ pA. This value is close to 470 ± 40 pA, the median value of the short-lived current blockades measured at a transmembrane potential of +150 mV (Supporting Information, Table S1 and Fig. S5). It is also notable that the amplitude of the current blockades (ΔI_b) of the short-lived events is diminished, because the events are near the time resolution of the instrument.27 Therefore, they are altered by the rise time of the filter.

The long-lived captures of BSA proteins

Long-lived current blockades occurred at every nanopore diameter greater than 8 nm and showed several general attributes across the investigated range. Significantly, unlike the short-lived current blockades, the long-lived events did not show a simple linear relationship with the BSA concentration. Instead, long-lived current blockades had a sudden onset that

occurred between low (10 nM) and high (180 nM) concentrations of BSA. The concentration at which such onset occurred did not appear to be affected by the diameter of the nanopore (Supporting Information, Table S2). For example, measurements on nanopores from 9 to 12 nm in diameter had onsets varying from 10 nM BSA to 180 nM BSA. On the other hand, nanopores from 14 to 16 nm in diameter had onsets as low as 20 nM BSA and as high as 180 nM BSA. While the onset of events could occur between these ranges, it was much more probable at high BSA concentrations. For nanopores with diameters between 12 and 16 nm, only 2 of 27 nanopores tested had an onset below 20 nM BSA, whereas 80% displayed long-lived current blockades at 180 nM BSA (Supporting Information, Table S2).

As expected, at very low BSA concentrations, the long-lived current blockades were rare. We tentatively interpret the "onset" of long-lived current blockades to be the adsorption of a single BSA molecule to the pore wall. The onset means that, at concentrations lower than the onset concentration, no BSA adsorbed to the pore surface within the timeframe of the experiment (10-minute single-channel electrical trace) and for the number of nanopores used in this work. Given the complexity of the nonspecific, random and spontaneous adsorption at the liquid-solid interface, involving a variety of electrostatic and hydrophobic forces, we think that a quantitative description, including model predictions of the far-from-the-equilibrium single-molecule events at very low BSA concentrations near the "onset" is quite difficult.

Thanks to the nonspecific nature of the BSA-nanopore binding interactions, the amplitude of the long-lived current blockades varied from nanopore to nanopore, indicating that different fragments of BSA produced such events in different nanopores (Supporting Information, Fig. S7). Moreover, the long-lived current blockades were typically smaller in amplitude than the short-lived current spikes, between 100 and 400 pA, at a transmembrane potential of +150 mV. The sudden onset of the BSA-produced, long-lived current blockades was often followed by a sudden cessation of such events, demonstrating that long-lived events occurred in a reversible fashion (Supporting Information, Fig. S8) and suggesting that these events were due to the adsorption of a single BSA molecule to the pore wall. The long-lived current blockades were either accompanied by additional current fluctuations between the resulting current state and a lower current state, with durations in the range of tens to hundreds of milliseconds (Fig. 2), or not accompanied by additional current fluctuations. The nature of gating for each event appeared to be different both for different nanopores and for different adsorption events within the same nanopore. If τ_{on} is the average inter-event time interval and τ_{off} is the average duration of the current blockade, then the apparent rate constants of association and dissociation are $k_{on}=1/\tau_{on}$ and $k_{off}=1/\tau_{off}$, respectively. The observed "on" rate constants were in the range 0.3 – 769.1 s^{-1} (n=9 experiments). The observed "off" rates were in the range 4.1 – 4170 s^{-1} (n=9). Moreover, we also observed multiple, subsequent and discrete current blockades at greater BSA concentrations, eventually producing the clogging of the nanopore (Supporting Information, Fig. S9).

Critical diameter of the nanopore for protein detection

We did not observe BSA-induced current blockades with nanopores narrower than ~8 nm in diameter. The hydrodynamic diameter of BSA at pH=7.4 is ~ 9 nm,23 close to the critical diameter (d_c=8 nm) that separated observable from non-observable BSA-produced current fluctuations. Our inability to probe BSA-induced current blockades with nanopores smaller than d_c is interpreted as the exclusion of proteins from the interior of the narrow nanopores. Recent experiments performed in this laboratory have shown that globular proteins with dimensions greater than the diameter of the nanopore produce no significant alterations in the unitary conductance or single-channel current fluctuations.28,29

In contrast, for nanopores whose diameter is 9 nm, the low-amplitude long-lived current blockades had a detectable effect on the frequency of the short-lived current spikes (Fig. 3). Thus, a single BSA molecule adsorbed to the interior of the nanopore produces a prolonged current blockade, creating an experimentally detectable energetic penalty for further BSA molecules to traverse the nanopore. The BSA protein that is attached to the surface decreases the effective diameter, reducing the frequency of the protein partitions into the nanopore interior. The trace in Fig. 3 is partitioned into four sections: A, B, C and D, which delineate the states of the long-lived current blockades. In state A, no long-lived current drop is observed (Fig. 3, A). A first long-lived current drop is observed at the beginning of state B. A counting of events was performed for each section using single-nanopore electrical data at a bandwidth of 10 kHz. At the beginning of state C, a second long-lived current drop occurs, accompanied by a drop in the frequency of short-lived current blockades from 32.2 ± 0.4 (Fig. 3, B) to 2.3 ± 0.3 s^{-1} (Fig. 3, C). At the beginning of state D, the current rises and the frequency of short-lived current spikes increases to 21.7 ± 0.4 s^{-1} (Fig. 3, D). For nanopores with a diameter much greater than 9 nm, very long-lived current blockades produced by single BSA proteins captured into the nanopore interior had no impact on the frequency of the large-amplitude, short-lived current blockades.

Voltage-dependence of the long-lived captures of BSA proteins

The frequency, amplitude and duration of long-lived current blockades, observed with a single 12 nm-diameter nanopore, were probed at voltages of +100 mV, +200 mV, +300 mV and +400 mV. Representative single-channel electrical traces are presented in Fig. 4. At progressively higher voltages, the probability of maintaining the lower state was increased, as judged by the longer-duration events recorded at this level. The probability of the open (upper) state was 0.71 ± 0.01 (n=1134 events), 0.38 ± 0.01 (n=3996), 0.26 ± 0.01 (n=614), and 0.12 ± 0.01 (n=24) at a transmembrane potential of +100, +200, +300, and +400 mV, respectively. An event-detection protocol was performed using ClampFit 10.2 (Axon) to count all current values above a threshold current. Each time the current passed above the threshold and then below, it was counted as an event. The sum of the duration of events above the threshold was taken and then this value was divided by the total sampling time. The free energy that is associated with the conformational fluctuation from the upper to the lower state could be estimated using the formula $\Delta G = -RT\ln(k_{off}/k_{on})$. The values for ΔG, at transmembrane potentials of +100, +200, +300 and +400 mV, were −0.24, −0.93, −1.66 and −4.30 kcal/mol, respectively. The total number of net negative charges of the BSA protein at pH 7.4 is 12.23 Assuming that only half of the charges are located on the protein domain that is attached to the Si_xN_y surface, then the corresponding electrical force that alters these switching fluctuations is 13.2 pN at a transmembrane potential of +400 mV. In this calculation, the electrical force is $F = neV/H_{eff}$ and the access resistance of the nanopore was taken into consideration.26 Here, n denotes the net number of negative charges that are not attached to the surface. It should be noted that this simple relationship between force and transmembrane potential is quite approximate, since it assumes a linear voltage drop across the nanopore length.

A cartoon representing the qualitative alterations in the dynamics of a single BSA protein attached to the Si_xN_y surface of the nanopore interior is shown in Fig. 4. The applied transmembrane potential alters the probability of the open state of the nanopore. In the absence of an electric field, there is a significant entropic barrier for the movable part of the BSA protein to partition into the interior of the nanopore (Fig. 4A), because more protein configurations are allowed in the aqueous phase than inside the nanopore. Therefore, the nanopore-BSA complex has a high probability to lie in the open state. However, the presence of a sufficiently intense electric field ($E \sim 7.5\times10^6$ V/m) tilts the energetic landscape along the force coordinate, lowering the activation free energy of the nanopore-

BSA complex to undergo a transition from the open state to the closed state, and increasing the probability of the movable negatively charged BSA protein to partition into the nanopore interior (Fig. 4B).

To test the reproducibility of the two-state gating, a set of experiments with nanopores ranging in diameter from 10 to 25 nm were used in the following conditions: 1M KCl, 10 mM potassium phosphate buffer at pH 7.4. BSA was added to the chamber to a concentration of 450 nM and a positive bias of +150 mV was applied. This high concentration of BSA was used to ensure the threshold for the onset of long-lived events was met. Long-lived events occurred in every nanopore at this concentration. Two-state gating occurred in 38% of the nanopores (n=13) tested within the 10 minute timeframe of the measurement (Supporting Information, Fig. S7). In those nanopores that showed two-state gating, the duration of the gating differed. The average duration of gating was 20 ± 15 sec, with values as short as 0.72 seconds and as long as 43 seconds.

DISCUSSION

In the last decade, protein adsorption on silicon nitride surfaces has been examined by a variety of experimental techniques, including electron microscopy,[30,31] ellipsometry,[32] florescent labeling,[7] and planar polarization interferometry (PPI).[33] In general, these approaches reveal surface organization and nonspecific, random adsorption phenomena of proteins at the liquid-solid interface.[4–6] In contrast, in this work we rely on the detectable single-channel current fluctuations produced by the interactions between single BSA proteins and the nanopore interior.

We interpret that the short-lived current blockades observed in the presence of BSA represent partition of individual proteins into the nanopore interior, but without a significant interaction with the Si_xN_y surface. The duration of the short-lived current spikes was close to the time resolution of our instrument (~15 μs).[27] This limitation precluded us from obtaining reliable voltage dependence data of the short-lived current blockades due to a large number of missed events at greater transmembrane potentials.[34] Assuming a two-barrier, one-well free energy landscape for the BSA partitioning into the nanopore, the voltage dependence would enable a rough estimate of the frequency of protein translocations from one side of the chamber to the other as well as the frequency of protein collisions with the nanopore entrance.[35] Remarkably, using an optimized chemiluminescence assay, Fologea and colleagues showed that the BSA proteins traverse nanopores with wide diameters of about 16 nm.[24] In this study, they also demonstrated the alteration of the BSA charge induced by pH modification near the pI of the protein.

The single-molecule measurements with BSA proteins carried out in this work also show that the solid-state nanopore might hold the potential for a rapid assay for determining the hydrodynamic radius of folded proteins in solution. We were not able to detect transient, short-lived current blockades with nanopores smaller than d_c=8 nm. However, we were able to detect current blockades with much shorter polypeptides using narrower nanopores. For example, we observed transient current blockades produced by NCp7, a 55 residue-long nucleocapside polypeptide of the HIV-1 virus, with solid-state nanopores in the range of 3–4 nm (Supporting Information, Fig. S10). Therefore, our inability to detect short-lived current blockades with nanopores smaller than d_c=8 nm was not caused by an experimental artifact.

We interpret that the long-lived current blockades represent strong binding events between the BSA protein and the Si_xN_y surface of the nanopore interior in the form of nonspecific, random and spontaneous protein adsorption. This interpretation relies on several lines of experimental evidence: (i) the dwell time of these biding events covers a very broad range,

from tens of milliseconds to several minutes; (ii) in some experiments, very long-lived discrete shifts in the unitary current of the nanopore were still persistent after BSA was removed from the chamber bath by perfusion. Such electrical signatures comprising step-wise changes of the single-channel current were not found within nanopores without BSA added to the chamber; (iii) binding events were strong enough that the application of a large reverse voltage (~750 mV) did not dislodge the protein from the nanopore. Very recently, Pedone and colleagues found similar long-lived captures of avidin proteins within the Si_xN_y -based synthetic nanopore,18 which differed from the short-lived ballistic flights of proteins through the nanopore. They interpreted that the long-lived events represent transient or semi-permanent adsorptions of avidin onto the interior surface of the nanopore. The dwell time for transient events was in the range of tens of milliseconds, whereas their amplitude was well defined.

In the case of long-lived current blockades with no further fluctuations, the BSA is in a stable conformation (Fig. 5A, **the top panel**). However when fluctuating, the BSA is likely in an unstable conformation, with only part of the BSA molecule adhering to the Si_xN_y surface (Fig. 5B, **the top panel**). We tentatively interpret that the fluctuating BSA protein undergoes conformational transitions between two states (Fig. 5B) and that these transitions are modulated by the transmembrane potential (Fig. 4). The typical transmembrane potential in this work was +150 mV, corresponding to an electric field of ~7.5×10^6 V/m. This electric field induces an overall force of ~14.4 pN on the 12 net negative charges of the BSA at pH 7.4.23 Prior force spectroscopy measurements have shown that proteins rupture at elongation forces of several pN.36 Therefore, we think that a force of 14 pN would be able to at least partially unfold the BSA proteins during their transit across the nanopore interior so that the proteins traverse the nanopore under various partially unfolded conformations. Recently, Talaga and Li proposed that the electrical forces present under physiologically pertinent applied transmembrane potentials can unfold the translocating proteins.25

We judge that the BSA molecules enter a flattened conformation upon nanopore wall adhesion, decreasing the excluded volume of the molecule. This accounts for the lower amplitude of the long-lived events as compared to the value that corresponds to the short-lived current blockades. Again, a linear dependence of the frequency of the short-lived current spikes on the BSA concentration in aqueous phase indicates that these short BSA-induced events cannot be attributed to nonspecific protein adsorption.

The decrease in the excluded volume of the BSA protein upon its adsorption to the silicon nitride surface is presumably caused by the loss of water around the portion of the polypeptide backbone attached to the solid surface. During nonspecific adsorption, it is likely that the BSA protein undergoes a conformational transition from a large-volume hydrophilic structure to a small-volume hydrophobic molecular structure.4،5،37 The hydrophilic structure is globular and highly hydrated, whereas the hydrophobic structure is “adsorption competent” and exhibits a smaller volume due to dehydrated groups in the BSA protein.1،2،4،5،37 This process is entropically driven due to the loss of structure (e.g., content of α-helix), which is triggered by the modification of the stabilizing hydrophobic contacts in the globular conformation in aqueous phase.9 Although, we observed that the amplitude of the long-lived current blockades (e.g., non-fluctuating states) is between 100 and 400 pA, at a transmembrane potential of +150 mV (Fig. 2B, Fig. 3, Fig. 5A), the two-state gating events (e.g., fluctuating states) are often higher, in the range of 200 – 900 pA (Fig. 5B; Supporting Information, Fig. S7). These values are consistent with our interpretation, since a partially adsorbed BSA protein is expected to have a larger accessible volume than a fully adsorbed BSA protein (Fig. 5).

BSA is a low-structural stability protein and generally tends to adsorb onto a broad variety of solid-state surfaces.37 The results obtained in this work confirm prior scanning electron microscopy,30 ellipsometry32 and interferometry33 studies of BSA adsorption on silicon nitride surfaces. Micic and colleagues have found that BSA in solution spontaneously adsorbed onto the surface of silicon nitride cantilevers of the AFM tips.30 This process continued until a uniform layer of proteins was formed over the surface of the tip. In general, proteins adsorb onto Si_xN_y surfaces more readily than to stoichiometric nitride films.32 Since the BSA-nanopore interaction is a non-equilibrium process, it would be instructive to assay macroscopic current measurements on an array of nanopores38 fabricated in a silicon nitride membrane. For example, individual long-lived bindings of BSA to the Si_xN_y surface, measured at the single-molecule level, could be observed by continuous decay in the macroscopic current flowing through the nanopore array. The rate of change of the macroscopic current might provide information about the apparent "adsorption" reaction rate constant. We anticipate that these kind of measurements will not only provide an estimate for the strength of the protein-surface interaction, but will also illuminate the nature of the adsorption process by revealing the experimental conditions in which the adsorption rate is substantially altered.

In the past, locking a polymer into a single nanopore and observing its partitioning into the nanopore interior,39,40 thermal fluctuations,41 temperature-induced conformational alterations,42 and interactions with various ligands11,20,22,43–45 have been pursued. Very recently, Lin and colleagues were able to lock a single-stranded RNA (ssRNA) molecule within the interior of the α-hemolysin (αHL) protein pore to probe its helix-coil transitions at the single-molecule level.46 Interestingly, they observed a much slower kinetic rate, nearly three orders of magnitude smaller than those rates measured in aqueous phase. This result is somewhat counterintuitive, since the confinement of biopolymers is known to catalyze their unfolding-folding transitions.47,48 Their finding might be determined by other experimental factors, such as the interaction of ssRNA with the hydrophilic side chains of the interior of the αHL protein pore. The paper of Lin and colleagues appears to share a similar approach with the design of the experiments presented in this work. For example, we are able to probe the nonspecific attachment of a single BSA protein within the interior of a solid-state nanopore and monitor conformational fluctuations of the tether in real time using time-resolved, single-channel electrical recordings.

The findings presented in this article suggest that caution must be practiced in the sensing of polypeptides with solid-state nanopores,16–18,24,49–54 in which there might occur various nonspecific interactions of different domains of the translocating proteins with the silicon nitride surface. One obvious way to overcome this challenge is the functionalization of the surface of the solid-state nanopore55,56 to prevent these long-lived captures of single proteins into the nanopore interior.

In summary, we show that the BSA proteins interact strongly with the Si_xN_y-based nanopores. Certainly, more experimentation is needed to decipher the different contributions to the adsorption of BSA proteins onto the interior surface of the nanopore. For example, the precise nature of the interaction between a BSA molecule and the Si_xN_y surface might be determined by obtaining the enthalpic and entropic contributions to the kinetic and thermodynamic constants, revealing information about which process in protein adsorption onto an inorganic surface is dominant. The long-lived captures differ in nature from the short-lived current spikes, which are attributed to protein excursions into the nanopore interior without a significant interaction with the nanopore surface. Moreover, the absence of transient BSA-induced current blockades with nanopores that feature a diameter smaller than 8 nm indicates that the hydrodynamic diameter of the BSA proteins, under the experimental conditions employed in this work, is ~8 nm. This finding is in excellent

agreement with prior experimental studies using electrophoresis NMR23 and solid-state nanopores.16

Supplementary Material

Refer to Web version on PubMed Central for supplementary material.

Acknowledgments

We are grateful to David Talaga, Khalil R. Howard, Andre Marziali and Vincent Tabard-Cossa for their help and stimulating conversations during the very early stage of these studies. We also thank Philip Borer for supplying the nucleocapside protein NCp7. The nanopore drilling was performed at the Electron Microscopy Facility of the Cornell Center for Materials Research (CCMR) with support from the National Science Foundation - Materials Research Science and Engineering Centers (MRSEC) program (DMR 0520404). The preparation of the silicon nitride membranes was performed at the Cornell NanoScale Facility, a member of the National Nanotechnology Infrastructure Network, which is supported by the National Science Foundation (Grant ECS-0335765). This work is funded in part by grants from the National Science Foundation (DMR-0706517) and the National Institutes of Health (R01 GM088403).

Reference List

1. Roach P, Farrar D, Perry CC. J. Am. Chem. Soc. 2006; 128:3939–3945. [PubMed: 16551101]
2. Roach P, Farrar D, Perry CC. J. Am. Chem. Soc. 2005; 127:8168–8173. [PubMed: 15926845]
3. Brewer SH, Glomm WR, Johnson MC, Knag MK, Franzen S. Langmuir. 2005; 21:9303–9307. [PubMed: 16171365]
4. Rabe M, Verdes D, Zimmermann J, Seeger S. J. Phys. Chem. B. 2008; 112:13971–13980. [PubMed: 18842014]
5. Rabe M, Verdes D, Rankl M, Artus GR, Seeger S. Chemphyschem. 2007; 8:862–872. [PubMed: 17387668]
6. Schon P, Gorlich M, Coenen MJ, Heus HA, Speller S. Langmuir. 2007; 23:9921–9923. [PubMed: 17711309]
7. Gustavsson J, Altankov G, Errachid A, Samitier J, Planell JA, Engel E. J. Mater. Sci: Mater. Med. 2008; 19:1839–1850. [PubMed: 18219554]
8. Haward SJ, Shewry PR, Miles MJ, McMaster TJ. Biopolymers. 2010; 93:74–84. [PubMed: 19728361]
9. Norde W, MacRichie F, Nowicka G, Lyklema J. J. Colloid Interf. Sci. 1986; 112:447–456.
10. Bezrukov SM. J. Membr. Biol. 2000; 174:1–13. [PubMed: 10741427]
11. Movileanu L, Howorka S, Braha O, Bayley H. Nat. Biotechnol. 2000; 18:1091–1095. [PubMed: 11017049]
12. Martin CR, Siwy ZS. Science. 2007; 317:331–332. [PubMed: 17641190]
13. Sackmann, B.; Neher, E. Single-Channel Recording. Second Edition ed.. Kluwer Academic/ Plenum Publishers; New York: 1995.
14. Li J, Stein D, McMullan C, Branton D, Aziz MJ, Golovchenko JA. Nature. 2001; 412:166–169. [PubMed: 11449268]
15. Dekker C. Nature Nanotechnology. 2007; 2:209–215.
16. Han A, Schurmann G, Monding G, Bitterli RA, de Rooij NF, Staufer U. Appl. Phys. Lett. 2006; 88
17. Han A, Creus M, Schurmann G, Linder V, Ward TR, de Rooij NF, Staufer U. Anal. Chem. 2008; 80:4651–4658. [PubMed: 18470996]
18. Pedone D, Firnkes M, Rant U. Anal. Chem. 2009; 81:9689–9694. [PubMed: 19877660]
19. Storm AJ, Chen JH, Ling XS, Zandbergen HW, Dekker C. Nat. Mater. 2003; 2:537–540. [PubMed: 12858166]
20. Zhao Q, Sigalov G, Dimitrov V, Dorvel B, Mirsaidov U, Sligar S, Aksimentiev A, Timp G. Nano. Lett. 2007; 7:1680–1685. [PubMed: 17500578]

21. Peters, P, Jr.. Serum albumin. In: Anfinsen, CB.; Edsall, JT.; Richards, FM., editors. Advances in Protein Chemistry. Academic Press, Inc.; London: 1985. p. 161-245.
22. Tabard-Cossa V, Wiggin M, Trivedi D, Jetha NN, Dwyer JR, Marziali A. ACS Nano. 2009; 3:3009–3014. [PubMed: 19751064]
23. Bohme U, Scheler U. Chem. Phys. Lett. 2007; 435:342–345.
24. Fologea D, Ledden B, McNabb DS, Li J. Appl. Phys. Lett. 2007; 91 nihpa38991.
25. Talaga DS, Li J. J. Am. Chem. Soc. 2009; 131:9287–9297. [PubMed: 19530678]
26. Hille, B. Ion Channels of Excitable Membranes. Third Edition ed.. Sinauer Associates, Inc.; Sunderland, Massachusetts, USA: 2001.
27. Colquhoun, D.; Sigworth, FJ. Single-channel recording. 2nd ed.. Sackmann, BNE., editor. Plenum Press; New York: 1995. p. 483-587.
28. Mohammad MM, Prakash S, Matouschek A, Movileanu L. J. Am. Chem. Soc. 2008; 130:4081–4088. [PubMed: 18321107]
29. Mohammad MM, Movileanu L. Eur. Biophys. J. 2008; 37:913–925. [PubMed: 18368402]
30. Micic M, Chen A, Leblanc RM, Moy VT. Scanning. 1999; 21:394–397. [PubMed: 10654425]
31. Grant AW, Hu QH, Kasemo B. Nanotechnology. 2004; 15:1175–1181.
32. Giannoulis CS, Desai TA. J. Mater. Sci: Mater. Med. 2002; 13:75–80. [PubMed: 15348209]
33. Shirshov YM, Snopok BA, Samoylov AV, Kiyanovskij AP, Venger EF, Nabok AV, Ray AK. Biosens. Bioelectron. 2001; 16:381–390. [PubMed: 11672652]
34. McManus OB, Blatz AL, Magleby KL. Pflugers Arch. 1987; 410:530–553. [PubMed: 2448743]
35. Movileanu L, Schmittschmitt JP, Scholtz JM, Bayley H. Biophys. J. 2005; 89:1030–1045. [PubMed: 15923222]
36. Best RB, Li B, Steward A, Daggett V, Clarke J. Biophys. J. 2001; 81:2344–2356. [PubMed: 11566804]
37. Rankl M, Ruckstuhl T, Rabe M, Artus GR, Walser A, Seeger S. Chemphyschem. 2006; 7:837–846. [PubMed: 16528782]
38. Kim M-J, Wanunu M, Bell CD, Meller A. Adv. Mater. 2006; 18:3149–3153.
39. Movileanu L, Cheley S, Howorka S, Braha O, Bayley H. J. Gen. Physiol. 2001; 117:239–251. [PubMed: 11222628]
40. Movileanu L, Bayley H. Proc. Natl. Acad. Sci. U. S. A. 2001; 98:10137–10141. [PubMed: 11504913]
41. Howorka S, Movileanu L, Lu XF, Magnon M, Cheley S, Braha O, Bayley H. J. Am. Chem. Soc. 2000; 122:2411–2416.
42. Jung Y, Bayley H, Movileanu L. J. Am. Chem. Soc. 2006; 128:15332–15340. [PubMed: 17117886]
43. Howorka S, Movileanu L, Braha O, Bayley H. Proc. Natl. Acad. Sci. U. S. A. 2001; 98:12996–13001. [PubMed: 11606775]
44. Howorka S, Nam J, Bayley H, Kahne D. Angew. Chem. Int. Ed Engl. 2004; 43:842–846. [PubMed: 14767954]
45. Nakane J, Wiggin M, Marziali A. Biophys. J. 2004; 87:615–621. [PubMed: 15240494]
46. Lin J, Kolomeisky A, Meller A. Phys. Rev. Lett. 2010; 104(158101)
47. Zhou HX, Dill KA. Biochemistry. 2001; 40:11289–11293. [PubMed: 11560476]
48. Takagi F, Koga N, Takada S. Proc. Natl. Acad. Sci. U. S. A. 2003; 100:11367–11372. [PubMed: 12947041]
49. Goodrich CP, Kirmizialtin S, Huyghues-Despointes BM, Zhu AP, Scholtz JM, Makarov DE, Movileanu L. J. Phys. Chem. B. 2007; 111:3332–3335. [PubMed: 17388500]
50. Wolfe AJ, Mohammad MM, Cheley S, Bayley H, Movileanu L. J. Am. Chem. Soc. 2007; 129:14034–14041. [PubMed: 17949000]
51. Movileanu L. Soft Matter. 2008; 4:925–931.
52. Movileanu L. Trends Biotechnol. 2009; 27:333–341. [PubMed: 19394097]
53. Kowalczyk SW, Hall AR, Dekker C. Nano. Lett. 2010; 10:324–328. [PubMed: 19902919]

54. Firnkes M, Pedone D, Knezevic J, Doblinger M, Rant U. Nano. Lett. 2010; 10:2162–2167. [PubMed: 20438117]

55. Wanunu M, Meller A. Nano. Lett. 2007; 7:1580–1585. [PubMed: 17503868]

56. Sexton LT, Mukaibo H, Katira P, Hess H, Sherrill SA, Horne LP, Martin CR. J. Am. Chem. Soc. 2010; 132:6755–6763. [PubMed: 20411939]

57. McManus OB, Magleby KL. J. Physiol. (Lond.). 1988; 402:79–120. [PubMed: 3236256]

58. Movileanu L, Cheley S, Bayley H. Biophys. J. 2003; 85:897–910. [PubMed: 12885637]

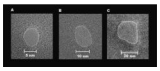

Figure 1.
Representative Si_xN_y nanopores imaged by a Technia F-20 S/TEM in TEM mode. The diameters of the nanopores were 5 nm (A), 10 nm (B), and 20 nm (C).

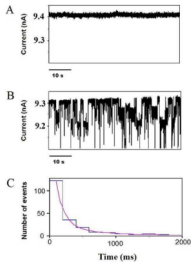

Figure 2.

Single-channel electrical recordings with a 12 nm-diameter Si_xN_y nanopore, revealing long-lived BSA captures. (A) A uniform, stable and fluctuation-free single-channel current was observed in the absence of the BSA protein. (B) Short-lived and long-lived gating current blockades were detected when 180 nM BSA was added to the *cis* side of the chamber. (C) The dwell-time histogram of the long-lived current blockades. The transmembrane potential was +150 mV. A two-exponential fit was made, giving time constants of τ_1=110 ± 11 ms and τ_2=440 ± 62 ms with the associated probabilities of P_1=0.58 ± 0.05 and P_2=0.42 ± 0.05, respectively. The fit was based upon a log likelihood ratio (LLR) test,[57,58] with a given confidence level of 0.95. The buffer solution contained 1 M KCl, 10 mM potassium phosphate, pH 7.4. For the sake of the clarity, the single-channel electrical traces were low-pass Bessel filtered at 400 Hz.

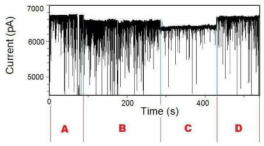

Figure 3.

Representative single-channel electrical recording with a 9 nm-diameter Si_xN_y nanopore. The electrical trace was low-pass Bessel filtered at 2 kHz. 10 nM BSA was added to the *cis* side of the chamber. The other experimental conditions were similar to those presented in Fig. 2.

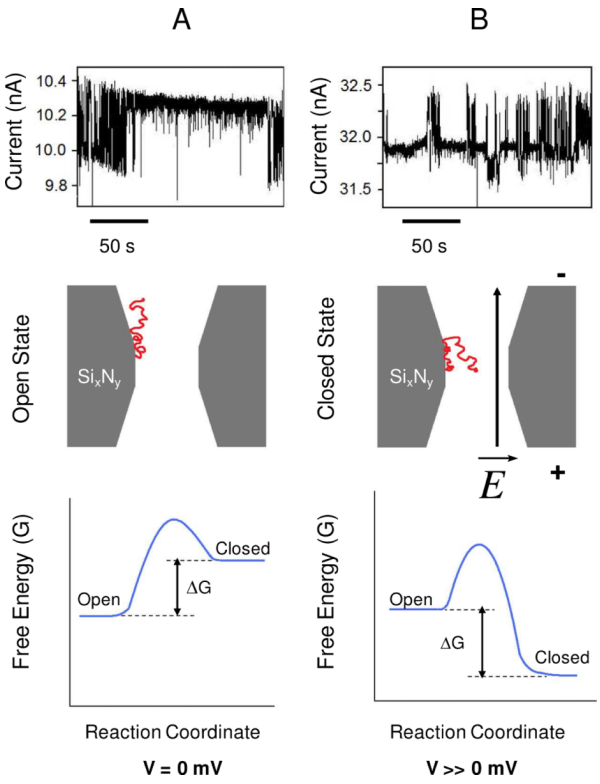

Figure 4.

The voltage dependence of the long-lived current fluctuations. The single-channel electrical traces from the top panels are recorded at +100 mV (A) and +300 mV (B). These experiments were carried out with a 12 nm-diameter nanopore. The BSA concentration in the *cis* chamber was 20 nM. The middle panels represent a schematic model of the voltage-dependent partitioning of the negatively charged, unattached part of the BSA protein into the nanopore interior at a transmembrane potential V=0 mV (A) and V >> 0 mV (B). These panels show the attached BSA protein in the open (A) and closed (partitioned) (B) states, respectively. The bottom panels illustrate free energy landscapes of the BSA-nanopore complex at zero (A) and much greater than zero (B) voltages, respectively. The other experimental conditions were similar to those presented in Fig. 2.

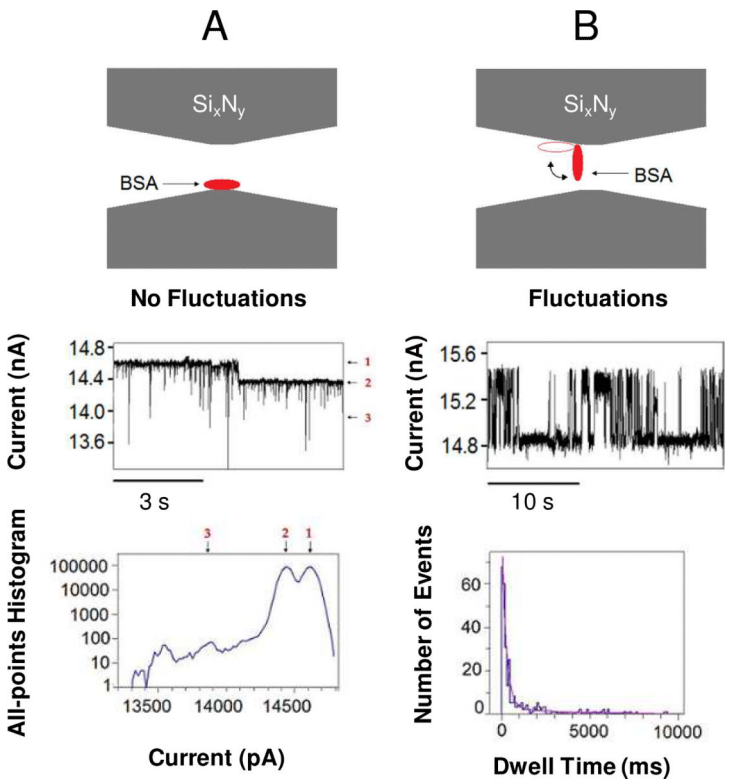

Figure 5.

Diagrams show the proposed mechanism for the long-lived protein captures. The upper panels indicate the position of adsorbed BSA (red) within the nanopore interior (grey), in cross-section. (A) BSA is attached within the interior of the nanopore causing a long-lived current blockade (middle panel) without additional long-lived current fluctuations of the resulting current state. The short-lived current spikes were in a sub-millisecond range. 20 nM BSA was added to the *cis* chamber; (B) BSA is attached to the nanopore interior, but in a different orientation than in (A). Additional current fluctuations occur (middle panel) in which a movable "unattached" part of the BSA protein wiggles between the nanopore interior and the aqueous phase, while the other end remains attached to the Si_xN_y surface of the nanopore interior. This results in a gating of the current between the open and the partially occluded (closed) state (Fig. 4). The left-hand bottom panel presents an all-points amplitude histogram of the trace in (A). The right-hand bottom panel is a dwell time histogram of the trace in (B), with $\tau_{off\text{-}1}$=240 ± 6.9 ms (P_1=0.70 ± 0.02) and $\tau_{off\text{-}2}$=3020 ± 730 ms (P_2=0.31 ± 0.04). 60 nM BSA was added to the *cis* chamber. The fit was based upon a log likelihood ratio (LLR) test,[57,58] with a given confidence level of 0.95. The diameter of the nanopore was 15 nm, as judged by the least square linear fit to an I–V curve (Supporting Information, Fig. S2). The other experimental conditions were similar as those presented in Fig. 2.